

*Supplement of*

# **Instability of Northeast Siberian ice sheet during glacials**

**Zhongshi Zhang et al.**

*Correspondence to:* Zhongshi Zhang (zhongshi.zhang@uni.no) and Qing Yan (yanqing@mail.iap.ac.cn)

## **1. Introduction to GRISLI**

GRISLI is a three-dimensional thermo-mechanical model, widely used in ice sheet modelling (Ritz et al., 2001; Charbit et al., 2007; Ganopolski et al., 2010; Colleoni et al., 2016; Wekerle et al., 2016). The equations are solved on a Cartesian grid (40 km×40 km) and with a semi-implicit temporal scheme and a point relaxation method. The model uses SSA to calculate the ice flow resulting from internal deformation in the grounded part of the ice sheet, and also the ice flow through ice shelves. It predicts the large-scale characteristics of ice streams using criteria based on the effective pressure and hydraulic load. As with PISM, GRISLI uses the same positive degree-day method for surface melting, with the same limits for PDD\_ice, PDD\_snow and Temp\_std. The melted snow is also able to refreeze at the same 60% proportion as PISM. A more comprehensive description of the model can be found in Ritz et al. (2001).

## **2. NorESM-BIOME4-PISM asynchronous coupled simulations with Maxi PISM parameters**

The PISM sensitivity experiments show that it generally takes 5 to 20 kyrs for PISM to reach quasi-equilibrium (Fig. S7), no matter which set of parameters is used. This result suggests that the swings of the two ice sheet configurations occur on the time scale of tens of thousands years. The time scale is independent of which PISM parameters are chosen. However, in some cases, for example P\_PiGlcV\_Maxi (Fig. S7c), the ice sheet does not totally disappear across NE Siberia, indicating one possible uncertainty in whether the simulated alternation of the ice sheet configuration is influenced by the selection of PISM parameters.

To exclude this uncertainty, we further repeat four NorESM-BIOME4-PISM asynchronous-coupled experiments, using the Maxi set of PISM parameters (Table S1). These experiments again illustrate the alternation of ice sheet configurations (Fig. S8). Although the

simulated ice volume depends on the PISM parameters, the simulated alternation of ice sheet configurations is independent of the chosen PISM parameters. With the Maxi set of parameters, the changes in atmospheric circulation and SST resulting from the higher and larger NE Siberian and Cordilleran ice sheets, are strong enough to induce ice sheet melting by themselves.

#### **4. Sensitivity experiments to different orbital parameters and greenhouse gas levels**

In order to test if the appearance of circum-Arctic ice sheet configuration depends on the chosen Earth orbital parameters and/or greenhouse gas levels, we carry out six sensitivity experiments. In addition to the idealized orbital parameters and greenhouse gas levels, we choose other three sets (Berger and Loutre, 1991; Petit et al., 1999) from 114 kyr (in MIS5d), 93 kyr (in MIS5b) and 70 kyr (in MIS4), respectively. With these three sets, we repeat PiGlc\_II and PbGlc\_II with the NorESM-L. Then, we use the resulting glacial climatology to force PISM. All these six experiments produce the circum-Arctic ice sheet configuration (Fig. S9), though the simulated ice volumes and shapes are different. These sensitivity experiments indicate that changes in atmospheric circulation are weak, when only forced with orbital parameters and greenhouse gas levels. In a glacial climate, vegetation feedbacks due to the expansion of tundra are important for the formation of the NE Siberian ice sheet.

#### **5. Sensitivity experiments with Bering Strait closed.**

In the circum-Arctic ice sheet configuration, the formation of the NE Siberian ice sheet can close the Bering Strait. We repeat the asynchronous-coupled experiments under the closed Bering Strait condition. These experiments (not shown here) still demonstrate the alternation between the two NH ice sheet configurations. Although the closing of the Bering Strait can influence SST in the North Pacific and the Arctic (Hu et al., 2010), this change in SST is too small to prevent the alternation of NH ice sheet configurations.

#### **6. Ice sheet experiments repeated with GRISLI**

In order to test if the alternation in the NH ice sheet configurations is specific to PISM alone, we carried out further ice sheet experiments using GRISLI. With GRISLI, we interpolate the simulated NorESM-L temperature and precipitation to a resolution of 40 km for the NH. Then we perform the same topography correction as PISM on the interpolated temperature using the ETOPO1 dataset, and the uniform lapse-rate correction of 7 °C/km, and the same correction as PISM on precipitation. Here, the basal melting of ice shelf is a function of ocean temperature (Álvarez-Solas et al., 2011).

$$bm = k * (To - Tf)$$

$k$  is chosen as  $0.5 \text{ m yr}^{-1} \text{ K}^{-1}$ ,  $T_o$  is the averaged ocean temperature between 0 to 300m.  $T_f$  is the freezing point temperature at the base of the ice shelf, which is dependent on the salinity and ice shelf depth beneath the ocean (Beckmann and Goosse, 2003).

$$T_f = 0.0939 - 0.057 * \text{salinity} + 7.64e - 4 * z_b$$

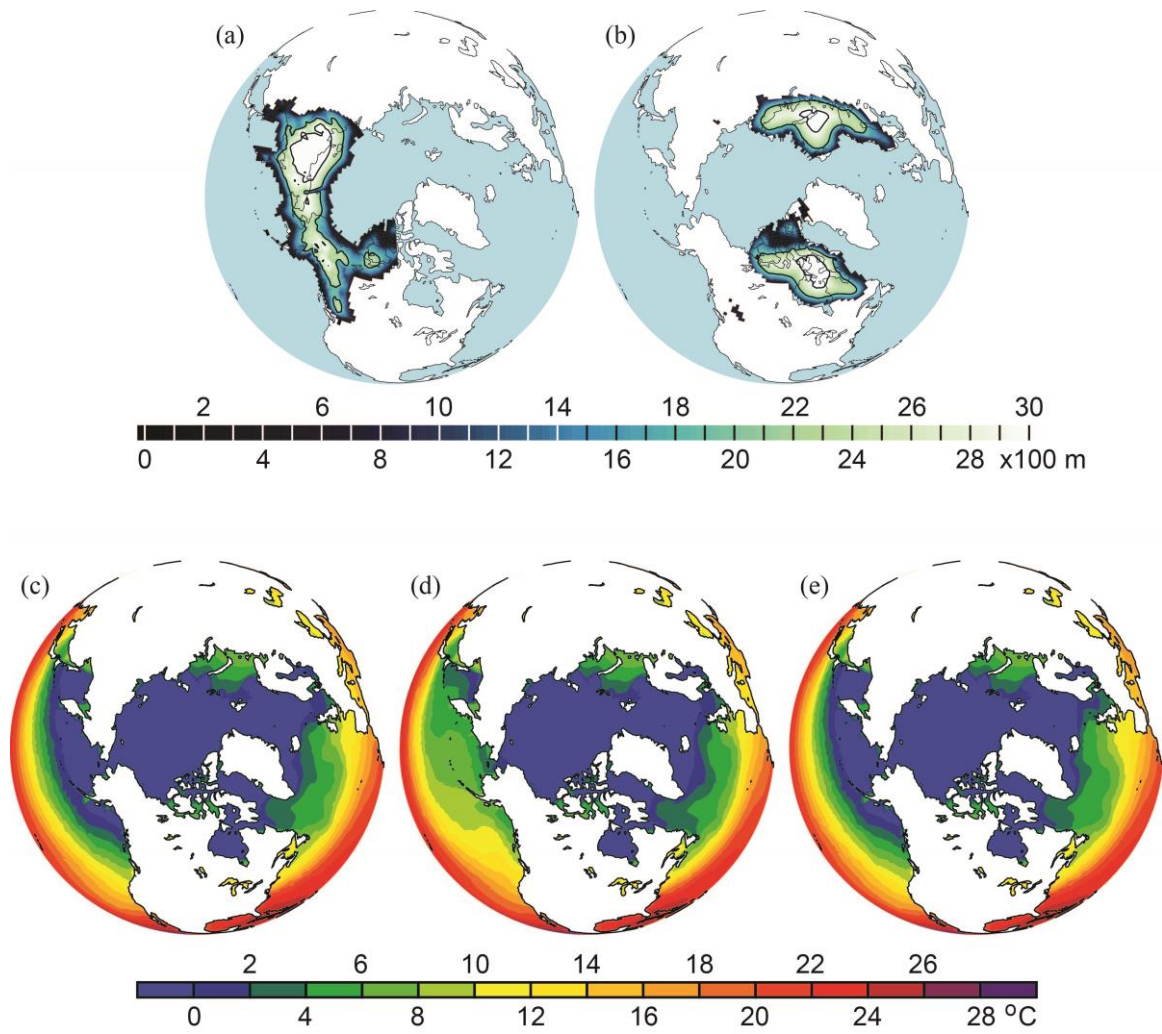
All GRISLI experiments are initialized from modern NH ice sheets and are run for 100 kyr to reach equilibrium.

With different internal model designs, GRISLI tends to overestimate the NE Siberian ice sheet. However, GRISLI also demonstrates the alternation between the two ice sheet configurations (Fig. S10), in good agreement with PISM, suggesting the simulated alternation in ice sheet configurations is independent of the ice sheet model used or the model parameters chosen.

## References

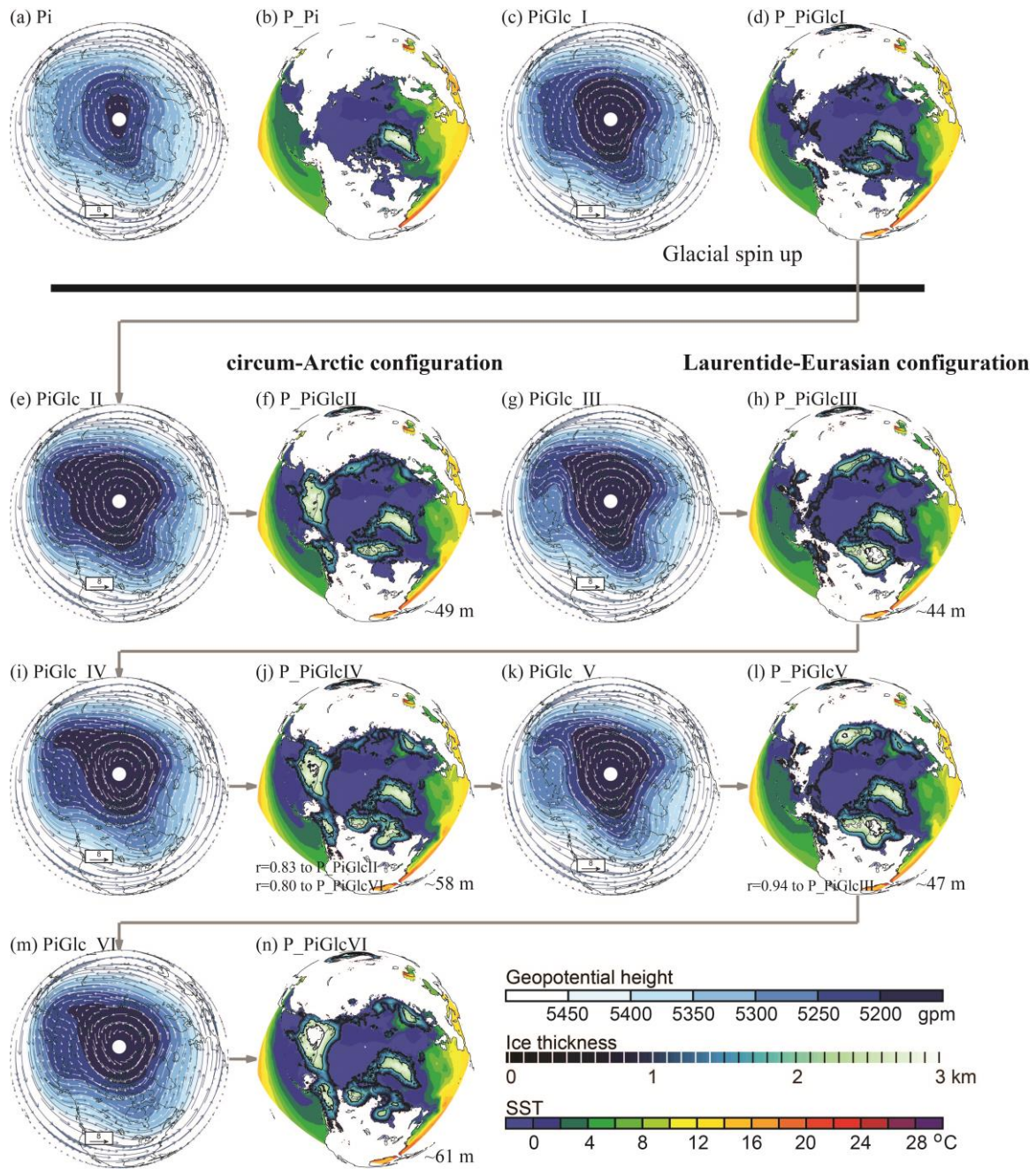
1. Álvarez-Solas, J., Montoya, M., Ritz, C., Ramstein, G., Charbit, S., Dumas, C., Nisancioglu, K., Dokken, T., Ganopolski, A., 2011. Heinrich event 1: an example of dynamical ice-sheet reaction to oceanic changes. *Clim. Past* 7, 1297–1306.
2. Beckmann, A., Goosse, H., 2003. A parameterization of ice shelf–ocean interaction for climate models. *Ocean modelling* 5, 157–170.
3. Berger, A., Loutre, M. F., 1991. Insolation values for the climate of the last 10 million years. *Quat. Sci. Rev.*, 10(4), 297–317.
4. Hu, A., Meehl, G. A., Otto-Bliesner, B. L., Waelbroeck, C., W., Loutre, M. F., Lambeck, K., Mitrovica, J. X., Rosenbloom, N., 2010. Influence of Bering Strait flow and North Atlantic circulation on glacial sea-level changes. *Nat. Geosci.* 3, 118–121.
5. Petit, J. R., Jouzel, J., Raynaud, D., Barkov, N. I., Barnola, J. M., Basile, I., Bender, M., Chappellaz, J., Davis, J., Delaygue, G., Delmotte, M., Kotlyakov, V. M., Legrand, M., Lipenkov, V., Lorius, C., Pépin, L., Ritz, C., Saltzman, E., Stievenard, M., 1999. Climate and Atmospheric History of the Past 420,000 years from the Vostok Ice Core, Antarctica. *Nature*, 399, 429–436.
6. Ritz, C., Rommelaere, V., Dumas, C., 2001. Modeling the Antarctic ice sheet evolution of the last 420 000 years: implication for altitude changes in the Vostok region, *J. Geophys. Res.* 106, 31943–31964.

Fig. S1



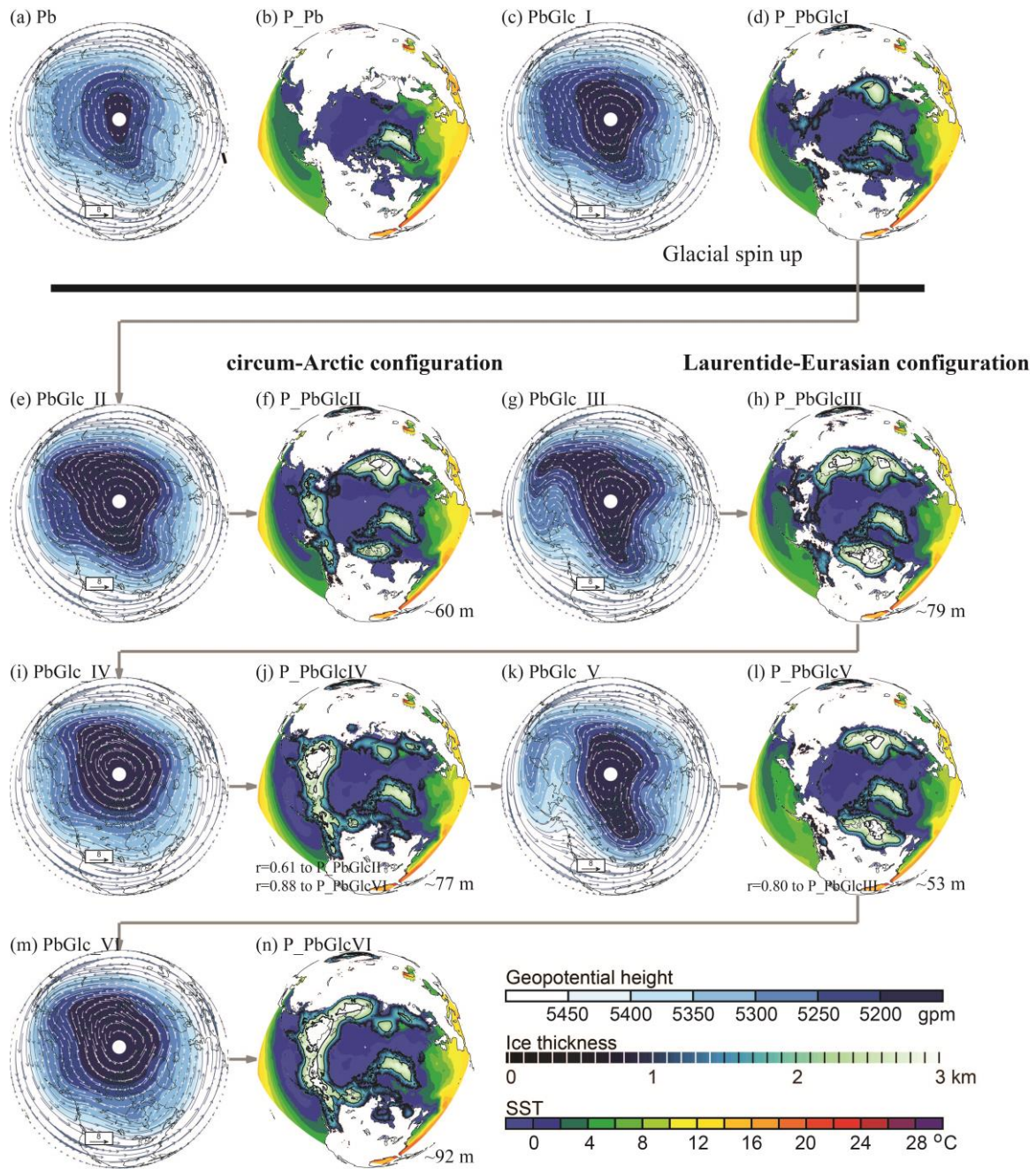
**Fig. S1: Boundary conditions used in CAM4 atmosphere-only experiments.** (a) anomalies for NE Siberian and Cordilleran ice sheets, (b) anomalies for Laurentide and Eurasian ice sheets, SST simulated in (c) PbGlc\_IV, (d) PbGlc\_V, (e) PbGlc\_VI coupled experiments.

**Fig. S2**



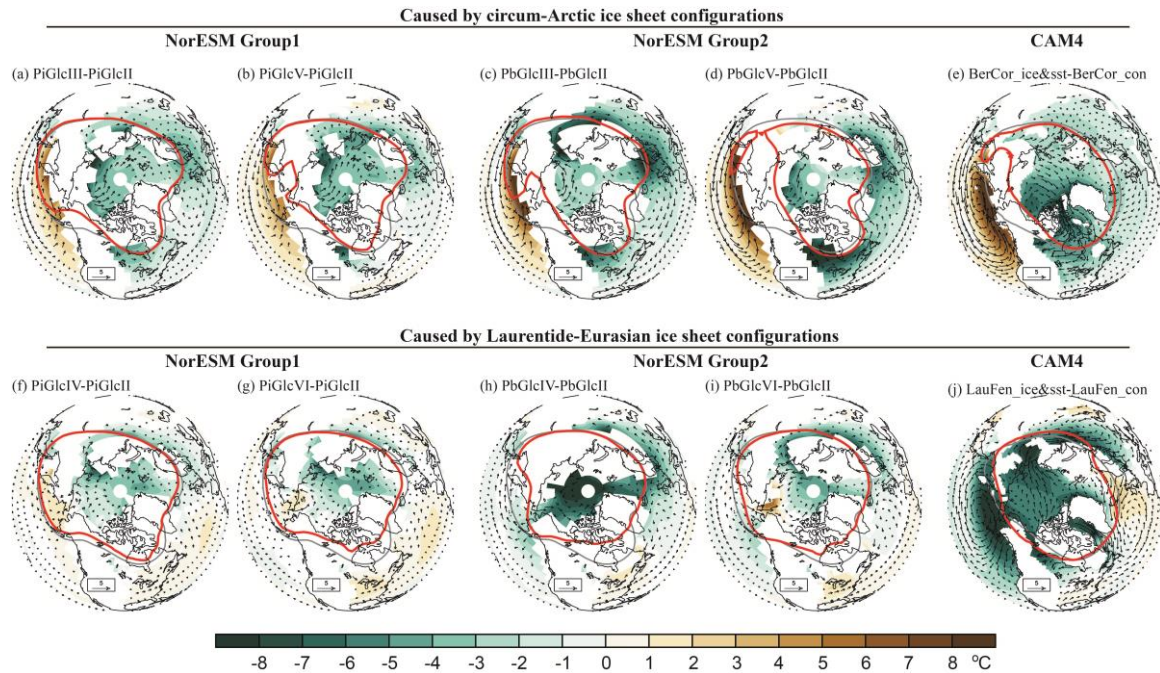
**Fig. S2: Atmosphere circulations and ice sheets simulated in NorESM-BIOME4-PISM asynchronous coupled experiments in Group 1.** (a), (c), (e), (g), (i), (k), (m) simulated annual mean 500hPa geopotential height (gpm) and winds (m/s). (b), (d), (f), (h), (j), (l), (n) simulated ice sheet configurations.  $r$  values show spatial correlation coefficients between simulated ice sheet configurations. Simulated ice volumes (equal to sea level drop, m) are illustrated at bottom-right corners of ice sheet configuration panels.

**Fig. S3**



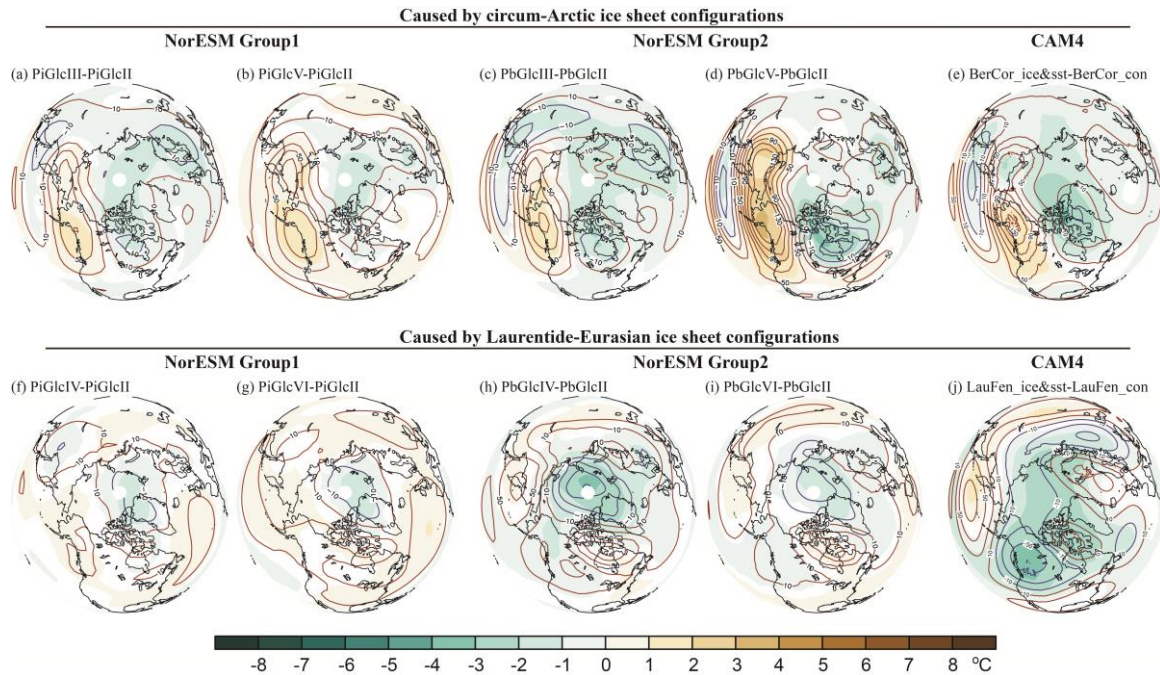
**Fig. S3: Atmosphere circulations and ice sheets simulated in NorESM-BIOME4-PISM asynchronous coupled experiments in Group 2.** (a), (c), (e), (g), (i), (k), (m) simulated 500hPa geopotential height (gpm) and winds (m/s). (b), (d), (f), (h), (j), (l), (n) simulated ice sheet configurations.  $r$  values show spatial correlation coefficients between simulated ice sheet configurations. Simulated ice volumes (equal to sea level drop, m) are illustrated at bottom-right corners of ice sheet configuration panels. Panel (j) and (l) are illustrated in Fig. 2.

**Fig. S4**



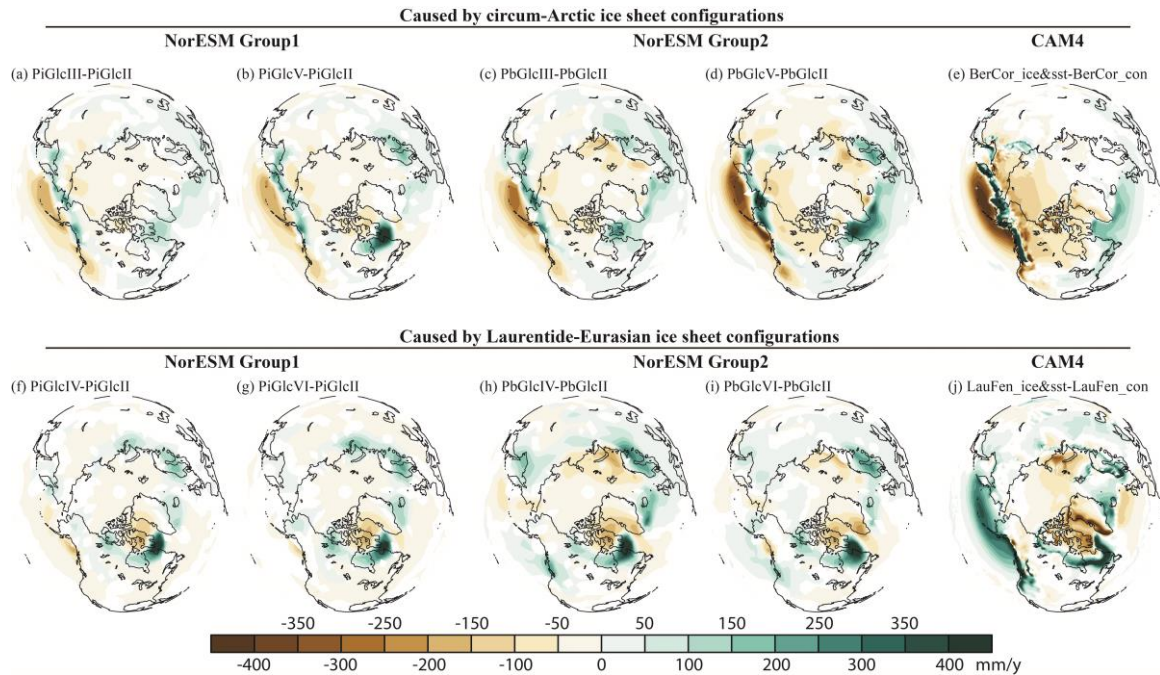
**Fig. S4: Changes in near-surface climate.** Upper panels: changes in annual mean near-surface temperature (shaded, °C), winds (arrows, m/s), and 500hPa geopotential height (red line, 5275 gpm) caused by the circum-Arctic ice sheet configurations, (a) and (b) for the two coupled experiments in Group1, (c) and (d) for the two coupled experiments in Group2, and (e) for the CAM4 atmosphere-only experiments. Lower panels: changes caused by the Laurentide-Eurasian ice sheet configuration, (f) and (g) for Group1, (h) and (i) for Group 2, and (j) for CAM4 experiments. The grey line shows the glacial reference 5275 gpm geopotential height, for NorESM group1, the glacial reference is PiGlc\_II; for NorESM group 2, the glacial reference is PbGlc\_II. Only changes in temperature that are significant at the 95% confidence level (two-tailed unequal t-test) are shown. Panel (d) and (i) are used in Fig. 2.

Fig. S5



**Fig. S5: Changes in 500hPa air temperature and geopotential height.** Upper panels: changes in annual mean 500hPa temperature (shaded, °C) and geopotential height (contours, gpm) caused by the circum-Arctic ice sheet configuration, (a) and (b) for the two coupled experiments in Group1, (c) and (d) for the two coupled experiments in Group2, and (e) for the CAM4 atmosphere-only experiments. Low panels: changes caused by the Laurentide-Eurasian ice sheet configuration, (f) and (g) for Group1, (h) and (i) for Group 2, and (j) for CAM4 experiments. The glacial reference is PiGlc\_II for NorESM group1. The glacial reference is PbGlc\_II for NorESM group 2. Only changes in temperature that are significant at the 95% confidence level (two-tailed unequal t-test) are shown.

**Fig. S6**



**Fig. S6: Changes in annual mean snow fall.** Upper panels: changes in annual snow fall (shaded, mm/y) caused by the circum-Arctic ice sheet configuration, (a) and (b) for the two coupled experiments in Group1, (c) and (d) for the two coupled experiments in Group2, and (e) for the CAM4 atmosphere-only experiments. Lower panels: changes caused by the Laurentide-Eurasian ice sheet configuration, (f) and (g) for Group1, (h) and (i) for Group 2, and (j) for CAM4 experiments. The glacial reference is PiGlc\_II for NorESM group1. The glacial reference is PbGlc\_II for NorESM group 2. Only changes that are significant at the 95% confidence level (two-tailed unequal t-test) are shown.

Fig. S7

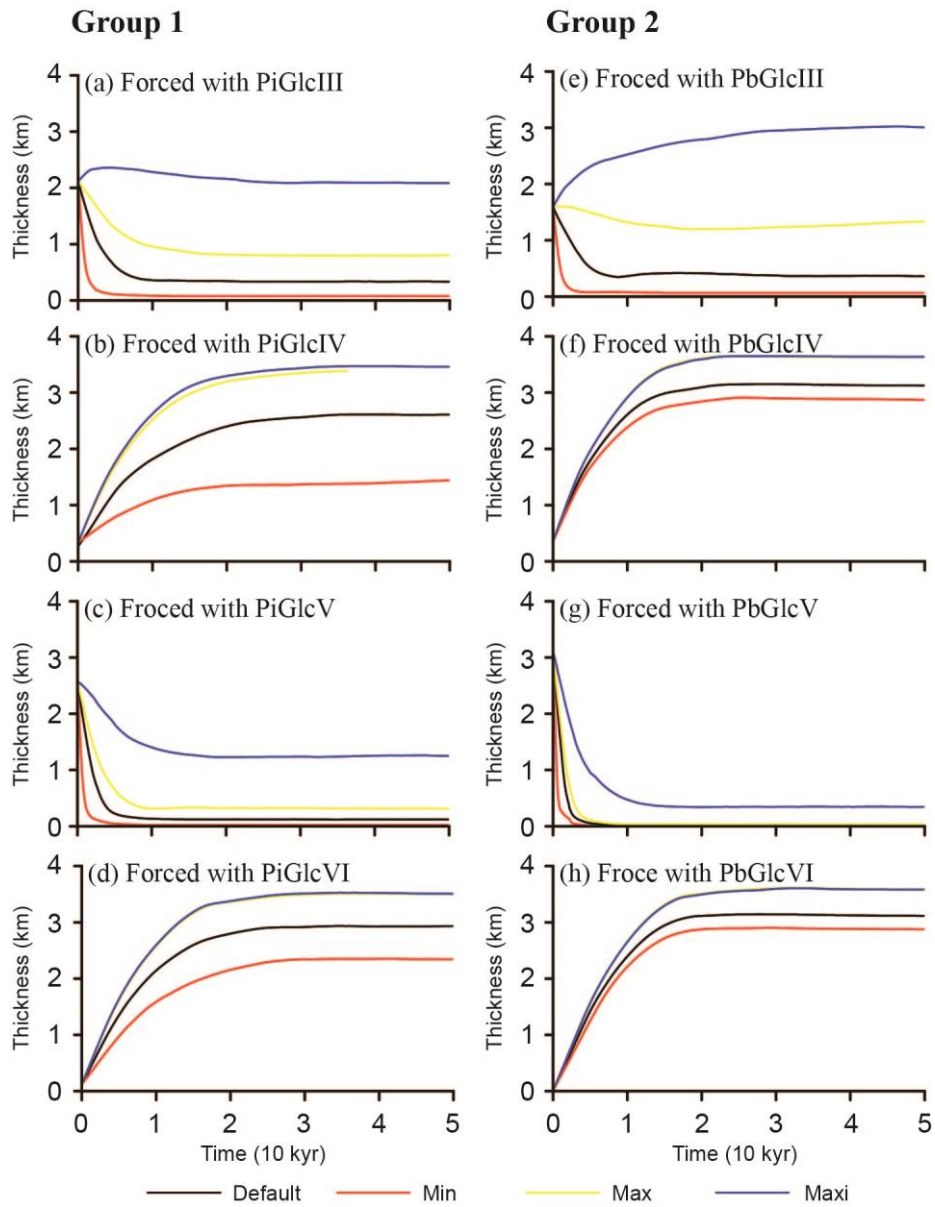
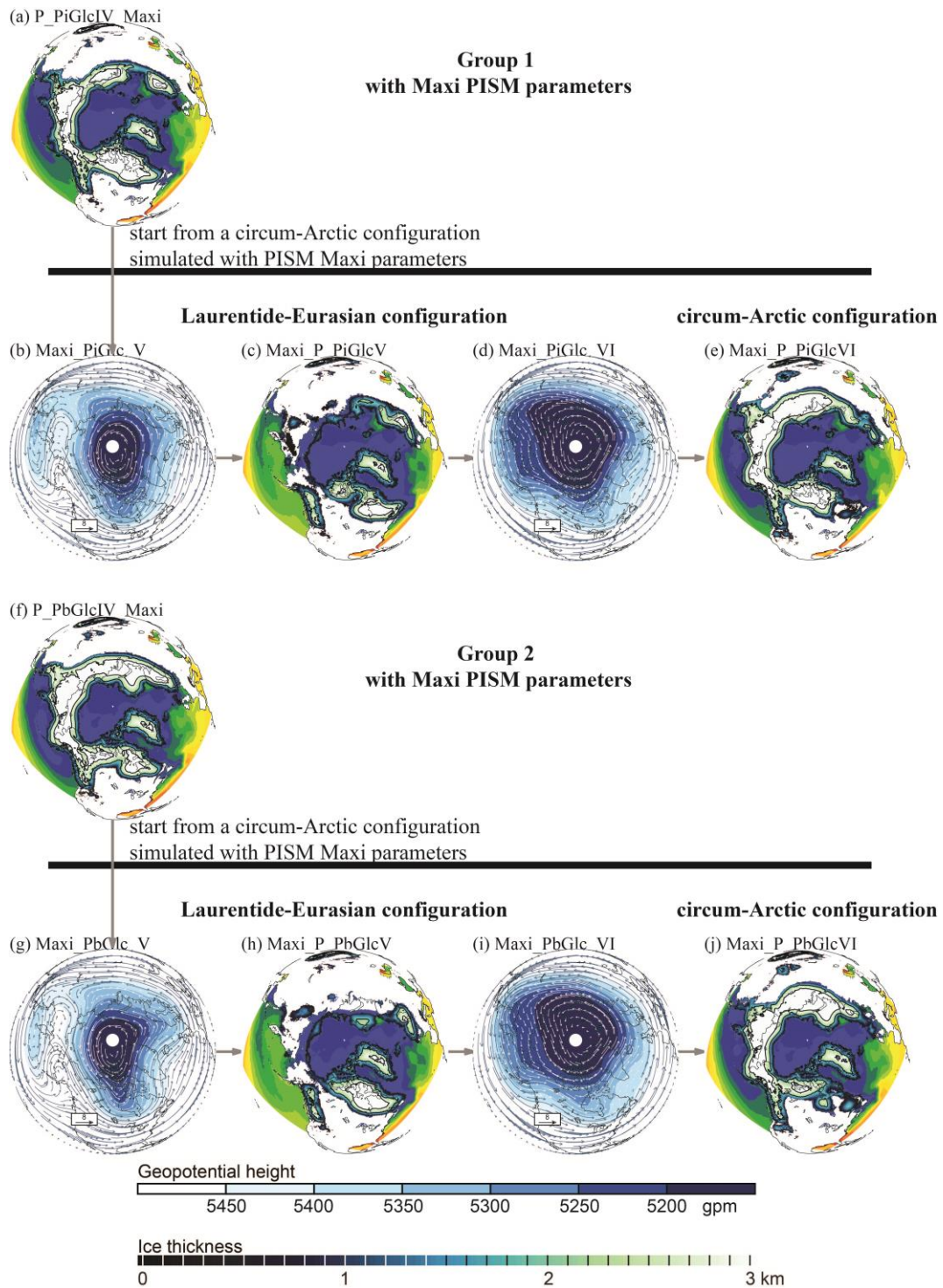


Fig. S7: Time series of ice thickness forced with four sets of PISM parameters. The ice thickness is averaged over the quadrilateral area marked in Fig. 2.

Fig. S8



**Fig. S8: Ice sheet configurations and atmosphere circulations simulated with the Maxi PISM parameters.** (a), (c), (e) PISM simulated ice sheet configurations, and (b), (d) NorESM-L simulated annual mean 500hPa geopotential height (gpm) and winds (m/s) for Group 1. (f) to (j) for Group 2.

Fig. S9

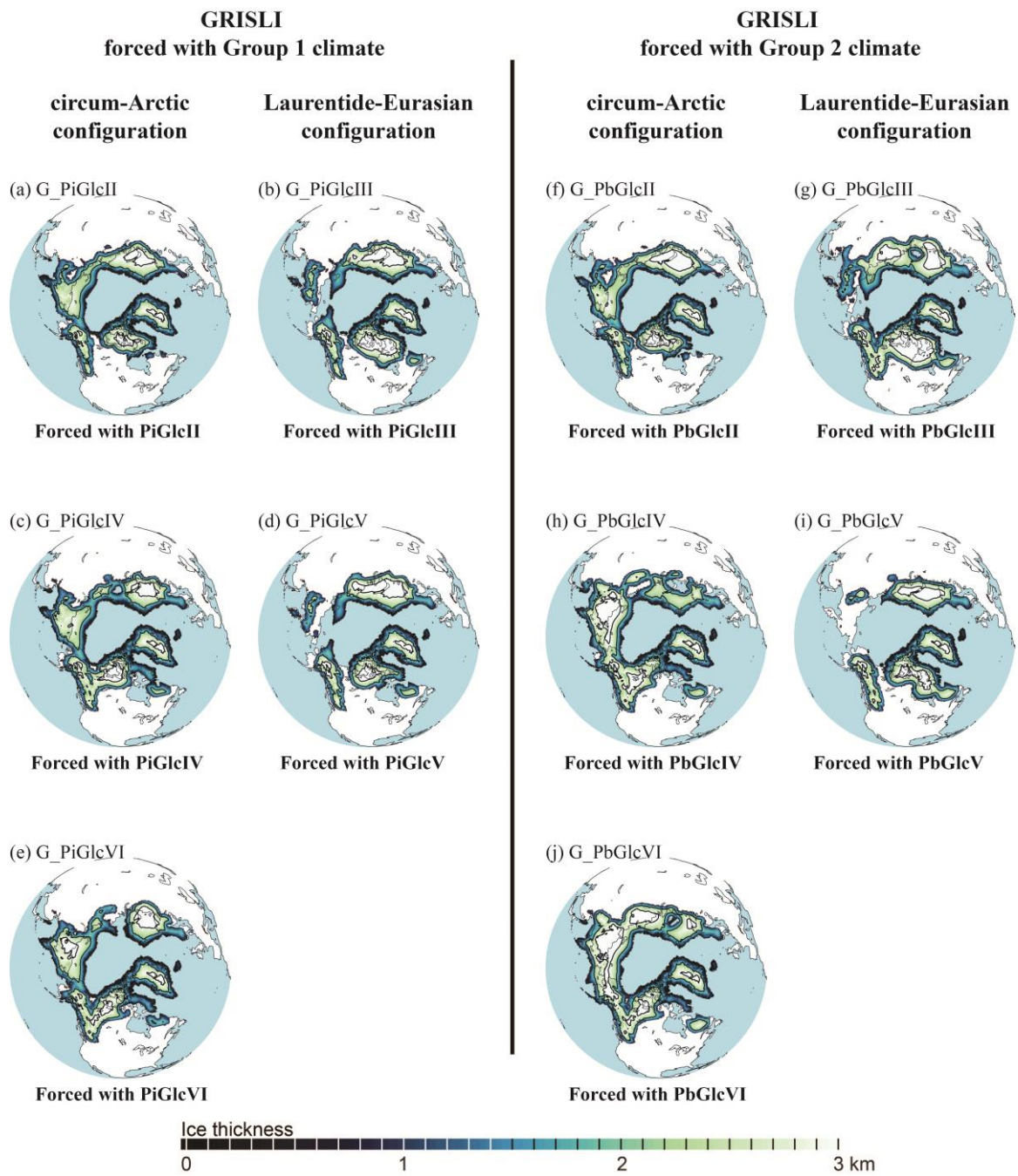
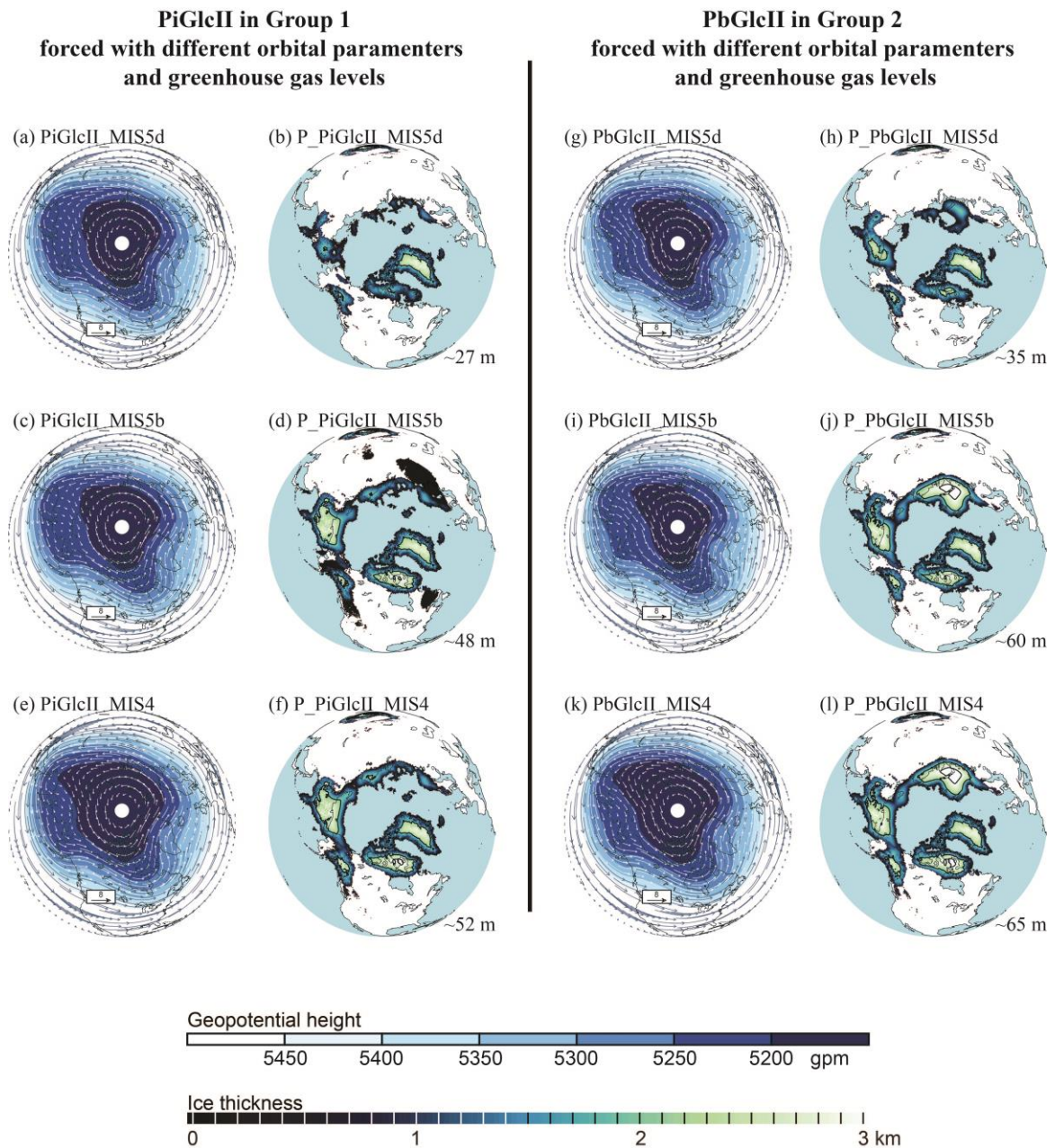


Fig. S9: Ice sheet configurations simulated with GRISLI. (a) to (e) for Group 1, (f) to (j) for Group 2.

Fig. S10



**Fig. S10: Atmosphere circulations and PISM Ice sheet configurations forced with MIS5d, MIS5b and MIS4 orbital parameters and greenhouse gas levels.** (a), (c), (e) NorESM-L simulated annual mean 500hPa geopotential height (gpm) and winds (m/s), (b), (d), (f) PISM simulated ice sheet configurations, for Group 1. (g) to (l) for Group 2.

Table S1. NorESM-BIOME4-PISM experiments with Maxi PISM parameters

Conditions	NorESM	Biome4	PISM
<b>Group 1: Modern land-sea distribution</b>			
Obliq. 22°, CO <sub>2</sub> 200 ppmv, B_PiGlcIV veg., P_PiGlcIV_Maxi ice	Maxi_PiGlc_V	B_PiGlcV	Maxi_P_PiGlcV
Obliq. 22°, CO <sub>2</sub> 200 ppmv, B_PiGlcV veg., Maxi_P_PiGlcV ice	Maxi_PiGlc_VI	B_PiGlcVI	Maxi_P_PiGlcVI
<b>Group 2: Barents Sea changed to land</b>			
Obliq. 22°, CO <sub>2</sub> 200 ppmv, B_PbGlcIV veg., P_PbGlcIV_Maxi ice	Maxi_PbGlc_V	B_PbGlcV	Maxi_P_PbGlcV
Obliq. 22°, CO <sub>2</sub> 200 ppmv, B_PbGlcV veg., Maxi_P_PbGlcV ice	Maxi_PbGlc_VI	B_PbGlcVI	Maxi_P_PbGlcVI

Table S2. Sensitivity experiments to different orbital parameters and greenhouse gas levels

NorESM	Eccen.	Obliq.	Prece.	CO <sub>2</sub> ppmv	CH <sub>4</sub> ppmb	PISM
<b>Group 1: Modern land-sea distribution</b>						
PiGlc_II_mis5d	0.0439	22.38	126.41	272.8	496.1	P_PiGlcII_mis5d
PiGlc_II_mis5b	0.0363	24.28	109.41	229.1	446.7	P_PiGlcII_mis5b
PiGlc_II_mis4	0.0235	22.35	110.35	211.9	444.3	P_PiGlcII_mis4
<b>Group 2: Barents Sea changed to land</b>						
PbGlc_II_mis5d	0.0439	22.38	126.41	272.8	496.1	P_PbGlcII_mis5d
PbGlc_II_mis5b	0.0363	24.28	109.41	229.1	446.7	P_PbGlcII_mis5b
PbGlc_II_mis4	0.0235	22.35	110.35	211.9	444.3	P_PbGlcII_mis4